JOURNAL OF GEOPHYSICAL RESEARCH, VOL. 93, NO. B4, PAGES 2839–2856, APRIL 10, 1988

Microplate and Shear Zone Models for Oceanic Spreading Center Reorganizations

JOSEPH F. ENGELN

Department of Geology, University of Missouri, Columbia

SETH STEIN, JOHN WERNER, AND RICHARD G. GORDON

Department of Geological Sciences, Northwestern University, Evanston, Illinois

The reorganization of oceanic spreading centers is often accomplished through the process of rift propagation. We first examine general rift propagation geometries for the simple two-plate case in which the propagating rift instantaneously reaches full spreading rate while the other rift dies instantaneously, such that the propagating and dying rifts never overlap. A velocity space representation provides a framework for describing the geometry of rift propagation and its various tectonic elements, and shows how both the failed rift and isochrons between the two rifts are reoriented as a consequence of purely rigid plate tectonics. We then discuss the more complex geometries that result when both growing and dying rifts spread simultaneously during propagation, such that a tectonically independent overlap region, like the Easter or Juan Fernandez plates along the East Pacific Rise, is produced. We examine the effect of the propagation rate and rise time of spreading on the evolution of overlap regions between dual oceanic spreading centers. The tectonics and evolution of such regions can be modeled by assuming that they act either as rigid microplates or as zones of distributed shear. Rigid plate models are suggested by the reasonable success of Euler vectors derived from inversions of plate motion data (spreading rates, transform azimuths, and slip vectors) both in describing available data and in predicting subsequently acquired data. On the other hand, recent structural data showing fabric oblique to the surrounding spreading centers might suggest shearing, rather than rigid behavior, in the interior of the Easter microplate. We use schematic evolutionary simulations for an Easter-style geometry to examine whether plate motion data and orientations of preexisting and present structures can be used to discriminate between rigid and shear models. In a microplate model, rigid plate tectonics requires that relative motion occur only along the boundaries of the overlap region, while structures within the overlap zone rotate rigidly. In contrast, in a shear model, relative motions at the boundaries differ from those predicted by rigid plate tectonics, and the angular relationships of structures within the overlap region are altered by internal deformation. Thus inversion of relative motion data yields different results for rigid and shear behavior. Similarly, under favorable circumstances, structural trends could be diagnostic of the different cases. We find that much of the Easter structural data suggestive of shearing are also consistent with rigid plate tectonics. We conclude that microplate models offer useful testable hypotheses for describing overlap systems and that shearing need be invoked only to explain features not describable by rigid plate tectonics. Furthermore, the approaches used here to study current overlap regions should be useful in the analysis of similar regions formed during past oceanic plate boundary reorganizations.

Rises and ridges are transient features...

H. W. Menard [1966]

INTRODUCTION

In a volume dedicated to H. W. Menard's memory, a natural beginning to a discussion of changes in oceanic spreading center geometry is with the observation that midocean ridges evolve. Figure 1, from *Menard et al.* [1964] demonstrates the existence of the Galapagos Rise, a bathymetric high east of the East Pacific Rise. The paper noted:

> Meager evidence suggests that the East Pacific Rise may be somewhat younger than the Galapagos Rise... The implications of the existence of the Galapagos Rise may be quite important with regard to the origin and history of oceanic rises and ridges... Adjacent parallel rises imply complications in the origin of oceanic rises which have not previously required explanation.

These prescient speculations are now accepted; the Galapagos Rise is considered a fossil spreading center formed during the evolution of the present East Pacific Rise [*Mammerickx et al.*, 1980]. One approach to studying the process of such evolution is to examine locations where spreading center geometry is now changing. Studies of such ridge-transform systems offer insights into the evolution of divergent oceanic plate boundaries. Here, we focus on sites where the relative motion between two major plates is divided between two spreading ridge systems separated by a tectonically independent overlap region. Such overlap regions, which occur on different scales and in various forms, are deviations from simple ridge-transform-ridge geometries and often provide the mechanism that transfers seafloor from one plate to another.

Dramatic examples occur along the East Pacific Rise near the location of the earth's fastest spreading. Bathymetric, seismic, and magnetic data suggest the existence of

Paper number 5B5825.
0148-0227/88/005B-5825$05.00

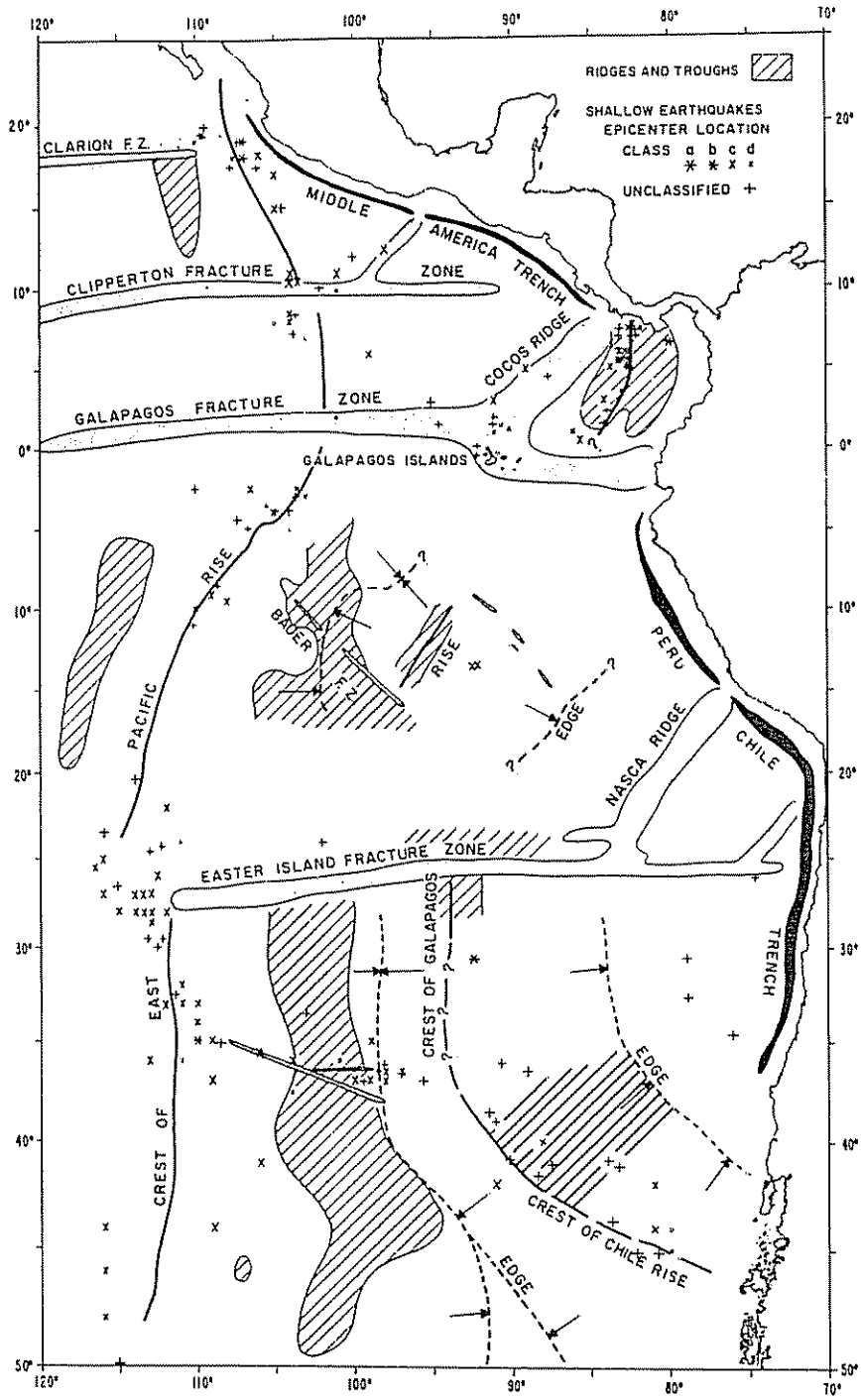

Fig. 1. Bathymetry and seismicity of the southeast Pacific [*Menard et al.*, 1964]. This paper documented the existence of the Galapagos Ridge and suggested that it predated the East Pacific Rise. This observation formed some of the earliest evidence for changes in spreading center geometry with time

dual spreading centers between the Nazca and Pacific plates at two places [*Forsyth*, 1972; *Herron*, 1972; *Anderson et al.*, 1974; *Handschumacher et al.*, 1981; *Craig et al.*, 1983; *Engeln and Stein*, 1984; *Naar and Hey*, 1985, 1986; *Schilling et al.*, 1985; *Hey et al.*, 1985; *Anderson-Fontana et al.*, 1986] Intriguingly, these two areas, the Easter and Juan Fernandez microplates, are distinguishable in Figure 1 as concentrations of earthquakes along the East Pacific Rise near 27°S and 34°S (Even more surprisingly, the seismicity of these microplates can also be identified, at least in hindsight, on the map shown by *Gutenberg and Richter* [1954]) Here, we refer to the Easter and Juan Fernandez "plates" even while discussing whether these regions can be treated as rigid

The growth of such overlap regions requires a finite time, because ridge segments do not extend their lengths infinitely fast and do not reach their full spreading rate instantaneously Thus overlap regions have various spatial scales Large features hundreds of kilometers wide, such as the Easter and Juan Fernandez plates, are generally

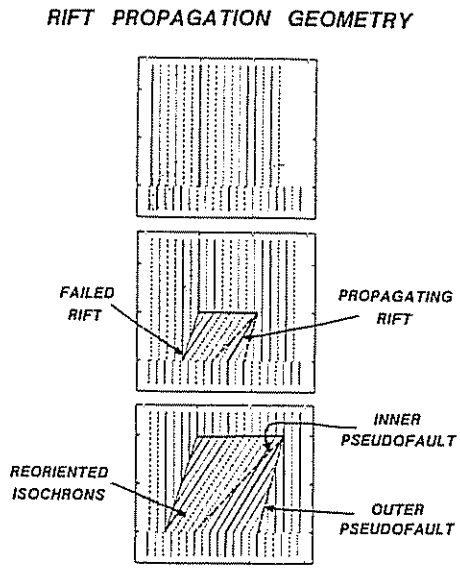

Fig. 2. Simple rift propagation geometry in which the propagating rift reaches full spreading rate instantaneously and the dying rift ceases instantaneously, with no overlap region forming between simultaneously spreading ridges. The plate on the left is shown by stippling. The pseudofaults bound seafloor formed on the growing ridge during propagation. Isochrons on the seafloor between the propagating and failed rifts, formed prior to rift propagation, are reoriented as they are transferred from the right plate to the left. This reorientation occurs by rigid plate tectonics.

considered microplates. They presumably evolve by rift propagation over millions of years, one ridge growing with time while the other is dying [*Hey and Vogt*, 1977; *Hey*, 1977; *Hey et al.*, 1980]. An intermediate scale (75 km) example has recently been identified in the Orozco Transform area [*Madsen et al.*, 1986]. Smaller, shorter-term features with scales of a few kilometers, termed overlapping spreading centers, are common along the East Pacific Rise [*Macdonald and Fox*, 1983; *Macdonald et al.*, 1984].

The identification of doubled magnetic anomalies formed during major boundary reorganizations that shifted seafloor from one large plate to another suggests that microplates were formed during these reorganizations [*Menard*, 1978; *Mammerickx et al.*, 1980; *Cande et al.*, 1982; *Okal and Bergeal*, 1983; *Rea and Dixon*, 1983; *Tamaki and Larson*, this issue]. Plate kinematics requires that an overlap region must have existed whenever the geologic record shows evidence of a ridge jump, unless (as seems unlikely) the newly formed ridge instantaneously reached full spreading rate along its full length, or the process occurred over time by rift propagation, with the propagating rift reaching full spreading rate immediately. Thus present propagating rifts and microplates can provide insights into the mechanisms of large-scale ridge boundary reorganizations.

If the formation of a dual ridge system is a local phenomenon which is a response to, and does not affect, the motion of the major plates, the overlap can take any form that preserves the rate and direction of relative motion between the two major plates. Any change in the rate or direction of motion on one of the overlap boundaries must be matched by a complementary change along the other ridge, unless yet another boundary comes into existence or the overlap region deforms. This basic kinematic constraint controls the evolution of all overlap systems. The rheology of lithosphere within the overlap affects the boundary evolution. Here we analyze this process, treating rift propagation and boundary evolution kinematically. The dynamics of the ridge propagation process have been discussed, using a fracture mechanics model, by *Phipps Morgan and Parmentier* [1985].

In this paper we review the kinematics of rift propagation and the resulting geometries of various tectonic elements for two plates with no overlap zone. We then discuss the formation and evolution of overlap regions using schematic models. These models, although simplified, provide insights into dual spreading centers and show some key features. The models are scaled in space and time to approximate the Easter plate, the best documented overlap zone, but are simplified to emphasize key elements. We discuss the tectonic evolution of overlap regions which act as rigid microplates and shear zones and investigate the use of relative motion and structural data to discriminate between the two types of models. We show the effect of propagation rate and rise time on the size, shape, and deformation of the overlap region.

RIFT PROPAGATION

Geometric Framework

Because many overlap systems are thought to have formed by rift propagation, we review some consequences of this process. In one simple form a new ridge segment propagates and preempts a preexisting ridge segment, with the locus of relative motion between the two plates instantaneously shifting from the dying to the growing ridge (Figure 2) [*Hey*, 1977]. The two ridge segment tips are joined by a boundary, usually taken to be a transform fault, which migrates with time. As the rift propagates, seafloor is transferred from one plate to the other. The precise geometry depends on the plate boundary geometry before propagation. For example, propagation may be initiated at a preexisting transform offset. Moreover, the direction and rate of propagation and spreading rate affect the geometry (Figure 3).

For simplicity, we assume that before propagation the offset ridge segments spread symmetrically and orthogonally at a half spreading rate u. From a point marked Z, the propagator tip P begins to move, at a velocity with components v parallel and w normal to the initial ridge trend. The resulting configuration is shown by the isochrons and the growing and dying rift orientations. The geometry of the propagator region depends on all three rates u, v, and w. Consider first the case where $u > w$. Since the propagator tip moves in the direction given by $\lambda = \tan^{-1}(w/v)$, oblique spreading generally occurs because the growing rift trend differs by λ from the normal to the spreading direction. The trends of the inner and outer pseudofaults, which enclose the seafloor formed on the growing ridge during propagation, are given by $\mu = \tan^{-1}[(u+w)/v]$ and $\epsilon = \tan^{-1}[(u-w)/v]$.

The geometry of the failed rift and transferred seafloor is independent of the ridge-normal component of the propagation velocity w. The failed rift trend is

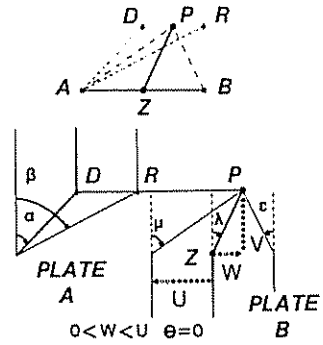

Fig 3. Geometry of a propagating rift and its representation in velocity space. Z is an origin fixed relative to the original ridge, P and D denote the propagating and dying rift tips, A and B are the two plates, and R represents the isochrons reoriented by rift propagation. Line ZP, with angle λ, gives the trend of the propagator; lines AP and BP, with angles μ and ϵ, give the trends of the inner and outer pseudofaults; line AD, with angle α, gives the trend of the dead rift, and line AR, with angle β gives the trend of the reoriented isochrons. The case shown is for orthogonal and symmetric spreading, with a half spreading rate u greater than the ridge-normal propagation rate w. The rift thus propagates into successively younger seafloor.

$\alpha = \tan^{-1}(u/v)$. The effect of seafloor transfer between the plates is shown by the orientation of originally ridge-parallel isochrons in the zone between the inner pseudofault and dead ridge. These isochrons are reoriented, or in *Searle and Hey's* [1983] terminology, sheared, to trends $\beta = \tan^{-1}(2u/v)$.

Such reorientation occurs by strictly rigid plate tectonics. The basic tenet of plate tectonics is that at any time, there is no relative motion between points on the same plate; relative motion occurs only between points on different plates. Although the boundary geometry can, and sometimes must, change, motion occurs only across plate boundaries. Thus this simple rift propagation model obeys rigid plate tectonics. The isochrons are reoriented only by motion across the transform fault, which migrates and hence time-transgressively offsets adjacent portions of isochrons.

These effects can be described in velocity space, using a geometric construction that provides the different angles (Figure 3, top). We use a frame of reference on a preexisting ridge segment, with origin Z, with x and y directions normal and parallel respectively to the preexisting ridge trend. (Equivalently, these directions can be viewed as normal and parallel to the doomed rift, since for simplicity all preexisting fabric is treated as the same.) The plates on either side move at the half rate u away from the ridge, which is stationary at point Z. Points A and B thus have coordinates $(-u,0)$ and $(u,0)$. The coordinates of the propagator tip P are its ridge-normal and ridge-parallel velocity components (w,v). As a result, line ZP in the velocity space figure is parallel to the growing rift, and makes an angle λ with the y direction. Similarly, lines AP and BP are parallel to the inner and outer pseudofaults, with angles μ and ϵ from the y direction. The dead rift and reoriented isochrons are represented by points D and R, with velocity space coordinates $(0,v)$ and (u,v). Thus lines AD and AR are parallel to these trends and have angles α and β from the y direction.

For a given ridge-parallel component of the propagation velocity v, the relative size of the half rate u and the ridge-normal component of the propagation velocity w yield interesting variations in geometry. As the velocity space representations show, for $u > w$ the rift propagates into successively younger seafloor, whereas for $w > u$ the rift propagates into successively older seafloor (Figure 4*a*). In the latter case the outer pseudofault angle ϵ is defined in the opposite sense relative to the y direction.

Two special cases are illuminating. If the ridge-normal component of propagation velocity equals the half rate ($w = u$), the rift follows an isochron, always breaking into seafloor of the same age (Figure 4*b*). The growing and failed rifts are parallel ($\lambda = \alpha$). The outer pseudofault parallels the unperturbed isochrons ($\epsilon = 0$), and isochrons reoriented by the propagation parallel the inner pseudofault ($\beta = \mu$). We have used a geometry of this type in discussing the Easter plate [*Engeln and Stein*, 1984].

If, instead, the propagation velocity has no ridge-normal

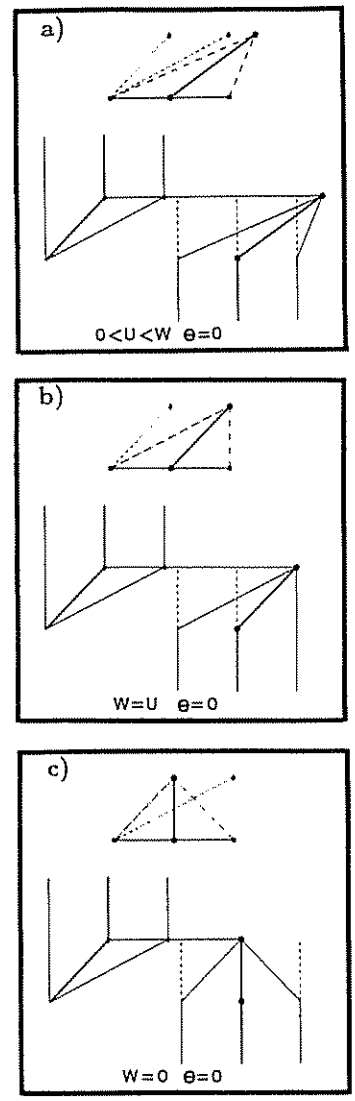

Fig 4. Propagating rift geometries which have the same half spreading rate u and an equal ridge-parallel propagation rate v, but different ridge-normal propagation rates w. (*a*) The rift propagates into successively older seafloor. (*b*) The rift propagates along an isochron. (*c*) The rift propagates parallel to the original ridge.

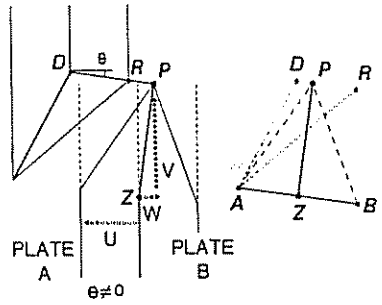

Fig 5. Propagating rift geometry where oblique spreading occurs prior to rift propagation. θ measures the obliquity and gives the direction of the transform connecting the rift tips. Spreading and propagation rates, and the various angles, are measured with respect to the prepropagation ridge geometry.

component ($w = 0$), the rift propagates parallel to the preexisting ridge ($\lambda = 0$), and orthogonal spreading occurs (Figure 4c). The rift breaks into successively younger seafloor. The pseudofaults have trends $\mu = \epsilon = \tan^{-1}(u/v)$, which is the same as the failed rift trend α, so the inner pseudofault parallels the failed rift. This geometry, formulated by *Searle and Hey* [1983, Figure 2a], is with some refinements similar to the propagator at 95.5°W on the Cocos-Nazca spreading center.

Specifically, *Searle and Hey* [1983] interpret the rift at that site as spreading orthogonally while propagating into seafloor formed by oblique spreading. They describe this using a variation on the geometry of Figure 4c, to account for the preexisting obliquity. This effect is also describable using rigid plate tectonics. The velocity space analysis can be applied, by measuring angles and propagation velocities relative to the initial oblique fabric and using the ridge-normal component of the half spreading rate. The angle θ between the ridge-normal direction and that of the connecting transform gives the obliquity (Figure 5). In velocity space, the plates are represented by points A and B with coordinates $(-u, u\tan\theta)$ and $(u, -u\tan\theta)$, and the propagator tip P is still (w, v). The dead rift and reoriented isochrons are given by points D and R, with coordinates $(0, v + w\tan\theta)$ and $(u, v + (w-u)\tan\theta)$. The corresponding angles for the different trends, given graphically by the velocity space figure, are:

$$\tan\alpha = u/(v + (w-u)\tan\theta),$$
$$\tan\beta = 2u/(v + (w-2u)\tan\theta),$$
$$\tan\lambda = (w/v),$$
$$\tan\mu = (u+w)/(v - u\tan\theta), \text{ and}$$
$$\tan\epsilon = (u-w)/(v + u\tan\theta).$$

The values shown in Figure 5 are similar to those used by *Searle and Hey* [1983, Figure 2b]. The orthogonal spreading cases (Figures 2-4) are simply ones with θ=0.

Thus given a range of propagation velocities and spreading rates, distinctive and complex structural patterns can be obtained from simple rift propagation and rigid plate tectonics. Figure 6 shows four different cases with the same spreading rate and different ridge-normal and ridge-parallel propagation velocities. The ridge-normal component of propagation velocity increases in successive panels, yielding propagation into successively younger (Figures 6a and 6b), the same age (Figure 6c), and successively older (Figure 6d) seafloor, which correspond to the cases in Figures 4c, 3, 4b, and 4a, respectively. The anomaly pattern is diagnostic of the different cases, which can be distinguished by the variation in the age of the seafloor immediately outside (to the right in the figure) the outer pseudofault, since this pseudofault marks the trace of the rift tip through the preexisting lithosphere. Moving toward the rift tip along the outer pseudofault, the lithosphere gets younger in the first two cases (Figures 6a and 6b), stays the same age in the third (Figure 6c), and gets older in the fourth (Figure 6d). Thus in all cases we use "younger" and "older" to denote ages relative to the present.

The two left panels show the same ridge-parallel propagation velocity, but in Figure 6a the ridge-normal velocity is zero. The trends of the reoriented isochrons and failed rift, which are independent of the ridge-normal propagation velocity, are the same in these two cases but the pseudofault and growing rift geometries differ. In contrast, in cases b through d, the ratio of ridge-normal and ridge-parallel propagation velocities is constant so the growing rifts have the same trend, but the trends of the reoriented isochrons, the failed rift, and the pseudofaults differ. In the figure, propagation begins at a preexisting transform, so the zone of reoriented isochrons has finite width at its southern limit, corresponding to the length of the preexisting transform. If the transform offset were small (or zero) this zone would be wedge shaped, as in the case shown by *Hey et al.* [1980].

Refinements

Greater complexities have been suggested. The evolution of a region can be affected by multiple propagation episodes [*Hey and Wilson*, 1982; *Wilson et al.*, 1984]. Moreover, *Hey et al.* [1980] suggest that a shear zone of finite extent separates the growing and dying rifts at the 95.5°W site. A finite overlap region forms when both ridges are simultaneously active, as occurs if a finite "rise time" is needed for all spreading to be be transferred from the dying to the growing rift. The size of the overlap region depends on the propagation rate and rise time [*Engeln and Stein*, 1984]. A shear zone, one of the possible geometries, is suggested by curvature of isochrons in the overlap region. Since rigid plate tectonic models require discrete plates within which no relative motion occurs, separated by boundaries across which all relative motion occurs, such models cannot describe a zone of distributed shear. Analytic expressions for a zone of simple shear in the spreading direction, corresponding to the geometry in Figure 4c, are given by *McKenzie* [1986].

The simple propagator geometries (Figures 2-6) can be viewed as degenerate cases of an overlap system, in which the overlap has zero area, since spreading starts and stops on the growing and failing rifts instantaneously. Consider three end-member models of the overlap region: a rigid plate, a shear zone, and an extensional zone (Figure 7). For simplicity, motions on the overlap region's boundaries are assumed parallel to those between the major plates. In the rigid plate case, conventional plate tectonics strictly applies. A zone of simple shear, in which deformation is parallel to the spreading direction, can be regarded as the limit of closely spaced transform faults, whereas an extensional zone can be considered the limit of a series of closely

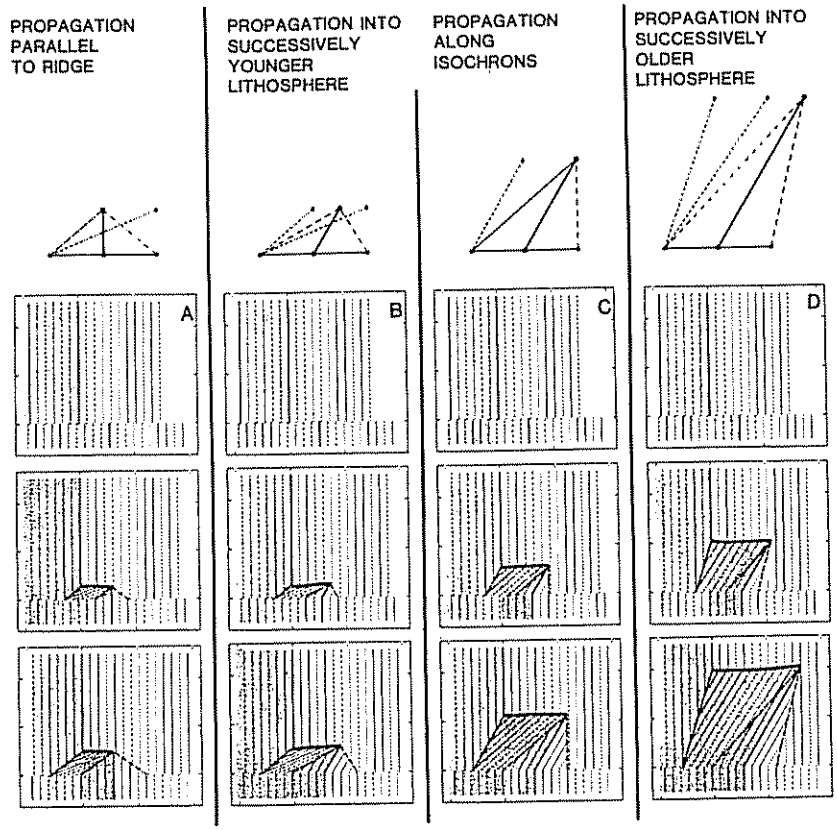

Fig. 6. Propagating rift geometries and the resulting isochrons. All cases have the same spreading rate but different propagation velocities. The ridge-normal component of propagation velocity increases in successive panels, yielding propagation into successively younger (Figures 6*a* and 6*b*), same age (Figure 6*c*), and successively older (Figure 6*d*) seafloor. Figures 6*a* and 6*b* have the same ridge-parallel propagation velocity, but in Figure 6*a* the ridge-normal velocity is zero. As a result, the reoriented isochrons and failed rift have the same trend in Figures 6*a* and 6*b*, but the propagator region geometries differ. In contrast, in Figures 6*b*-6*d*, the growing rift trend is similar, but the pseudofault, reoriented isochron, and failed rift trends differ.

spaced ridges or normal faults. The actual behavior of overlap regions may be any combination of these possibilities. Rigid plate models have been proposed for the Easter and Juan Fernandez plates on the basis of the distributions of seismicity [*Forsyth*, 1972; *Anderson et al.*, 1974] and relative motion studies [*Engeln and Stein*, 1984; *Anderson-Fontana et al.*, 1986]. Shear in the overlap region has been suggested for a propagating rift near the Galapagos [*Hey and Vogt*, 1977; *Hey et al.*, 1980, 1986]. *Courtillot* [1982] analyzed continental rifting and the subsequent initiation of seafloor spreading using a shear model.

The situation for extensional zones is less clear. Such models are commonly used in continental tectonics to describe regions like the Basin and Range. The oceanic analogy is less clear, although *Isezaki and Uyeda* [1973] suggested that diffuse spreading occurred in the Japan Sea. Thus although multiple overlapping ridges, corresponding in the limit to an extensional zone, are geometrically acceptable, none have been definitively observed in modern oceanic lithosphere. We therefore limit our discussion to dual ridge systems with either rigid plates or shear zones in the overlap region and explore the different consequences of these models for the evolution of a region like the Easter plate.

EASTER PLATE

Models of large overlap systems are conditioned by the observations and resulting ideas from the Easter plate, the best studied example. Since its identification [*Herron*, 1972; *Forsyth*, 1972], its tectonics and evolution have been studied by several investigators. *Anderson et al.* [1974] suggested that the region acts as a rigid microplate whose southern boundaries were spreading centers joined by long transforms to the East Pacific Rise to the north. *Handschumacher et al.* [1981] used magnetic data to interpret the eastern boundary as a propagator growing northward at the expense of the west ridge.

Recent studies follow this theme of microplate growth

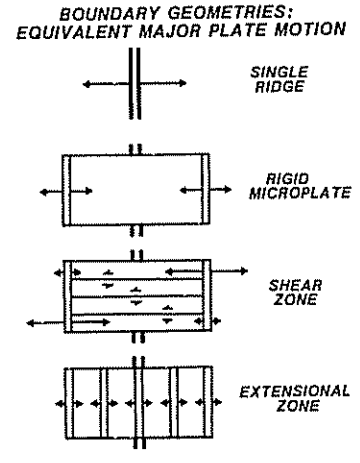

Fig. 7. Boundary geometries that yield the same relative motion between two major plates at a spreading center.

by rift propagation The hypothesis that the region behaves as a rigid plate, rather than a diffuse deformation zone, is suggested by the concentration of seismicity along the boundaries (Figure 8, top) Euler vectors for the motions between the Easter, Nazca, and Pacific plates can be determined by combining spreading rates from magnetic anomalies and azimuths of motion from bathymetry and earthquake focal mechanisms in a relative plate motion inversion that best fits the data in a least squares sense [*Chase*, 1972; *Minster et al.*, 1974] If the microplate is rigid, the data should be well fit Once Euler vectors are determined, relative motions can be predicted on portions of the boundaries where data are not yet available

Figure 8 (bottom) shows the results [*Engeln and Stein*, 1984] The proximity of the Nazca-Easter and Pacific-Easter poles allows significant variation in motion along the boundaries The model predictions are good; spreading rates decrease rapidly to the north along the east ridge The Pacific-Easter Euler vector fits the observed rate on the northwest boundary fairly well and predicts slow spreading on the southwest boundary These predictions agree with seismological observations: the southwest boundary is the most active seismically with normal faulting events suggesting slow spreading, by analogy to the Mid-Atlantic Ridge, whereas the strike-slip events suggest transform motion The transform direction implied by the strike-slip events on the southwest boundary is fit well, and spreading is predicted to be slightly oblique The northern boundary (or diffuse boundary zone) remains unclear, with the predicted motions changing from oblique convergence to strike-slip to oblique divergence The main constraint on the pole locations is the variation in rates along the growing ridge and the assumption of orthogonal spreading Addition of the slip vectors causes only minor changes in pole positions

These relative motions were determined using earthquake slip vectors [*Engeln and Stein*, 1984], marine magnetic data [*Handschumacher et al.*, 1981], and a boundary geometry inferred from the bathymetry [*Mammerickx and Smith*, 1978] Subsequent detailed magnetic and bathymetric surveys [*Hey et al.*, 1985; *Schilling et al.*, 1985; *Naar and Hey*, 1985; 1986] provide better descriptions of the plate's geometry Analysis of these data yields preliminary pole locations [*Naar and Hey*, 1985; D Naar, personal communication, 1986] similar to those determined with the earlier data, and suggests that the nature of the boundaries agrees with the predictions of the Euler vectors The similarity of poles and the successful predictions suggest that the Easter plate can be treated as a rigid microplate when studying present-day relative plate motions

The new data both allow a more accurate model and offer new insights They reflect the history of the boundary geometry which may have evolved in a series of rift propagation stages In addition to the magnetic data, which directly record the spreading history of various boundary segments, seafloor lineaments reflect both the history of boundary segments and the mechanical nature of the region between the growing and dying ridges *Hey et al.* [1985] note that Seabeam bathymetric data show trends in the plate interior oblique to the spreading center trends observed outside They suggest that the oblique trends result from the complex evolution of the overlap region, as seafloor in the microplate was transferred from the Nazca to the Easter plate Specifically, they propose that

> ...because of the time-progressive transferral of this lithosphere from one plate to another, the preexisting fabric of the transferred lithosphere was sheared and tectonically rotated into the observed oblique trends characteristic of continuous rift propagation... The scale of the microplate shearing is impressive...with shear deformation distributed over the entire plate ($\sim$ 400 $\times$ 400 km)...

We thus explore the evolution of Easter-style overlap systems for two end-members, a rigid microplate or a zone of simple shear, for which the region's boundaries and interior evolve differently Though an overlap region may not have been entirely rigid or pervasively sheared throughout its evolution, one of these types of behavior may dominate, although an intermediate combination of the "end member" cases may be most accurate

Two basic data types reflect the region's evolution First, the location of and relative motion on the boundaries provide both "instantaneous" relative motion data at any time, and an isochron history comparable to magnetic anomaly data These will be distinct for the end-member cases Second, various structural features that either predate or form during rift propagation reflect the region's history Because the rates and directions of relative motion change during rift propagation and death, the nature and orientations of these features record past relative motions and are diagnostic of the mechanics of the overlap region Preexisting structures within the overlap move passively while both ridges are active if the region is rigid, but are deformed if the region is pervasively sheared Thus structural features can be diagnostic of the mechanical behavior of the overlap region

RIGID PLATE MODEL

Figure 9 traces the development of a rigid plate between the propagating and dying ridges through five equal time increments Since the plate is rigid, no relative motion occurs between points within the microplate; relative motion occurs only at points on the boundaries For simplicity, a set of clarifying assumptions has been made The west plate is fixed, and the Euler pole for the two large plates is 90° away Spreading on these ridges is orthogonal, and all spreading is symmetric The initial configuration, two ridges offset by a transform, changes as propagation begins at time T_0 at the southeast ridge segment and continues until T_3, when propagation ceases As the growing ridge propagates into the major plate along an isochron, a convergent boundary moves with the tip, so seafloor is transferred from the east major plate to the microplate The spreading rate on the growing (east) ridge increases linearly with time, while spreading on the dying ridge slows at the same rate, so that points on the dying ridge become inactive as the corresponding points on the east ridge reach full rate As a result, the microplate rotates and the southern transform evolves into a slow and obliquely spreading ridge Time T_3 is the instant before the southernmost point on the west ridge ceases spreading and the southern boundary starts to migrate northward, transferring seafloor from the microplate to the major plate to the west Thus by T_4 one third of the overlap has been transferred between the large plates As the geometry of the northern and southern boundaries is not

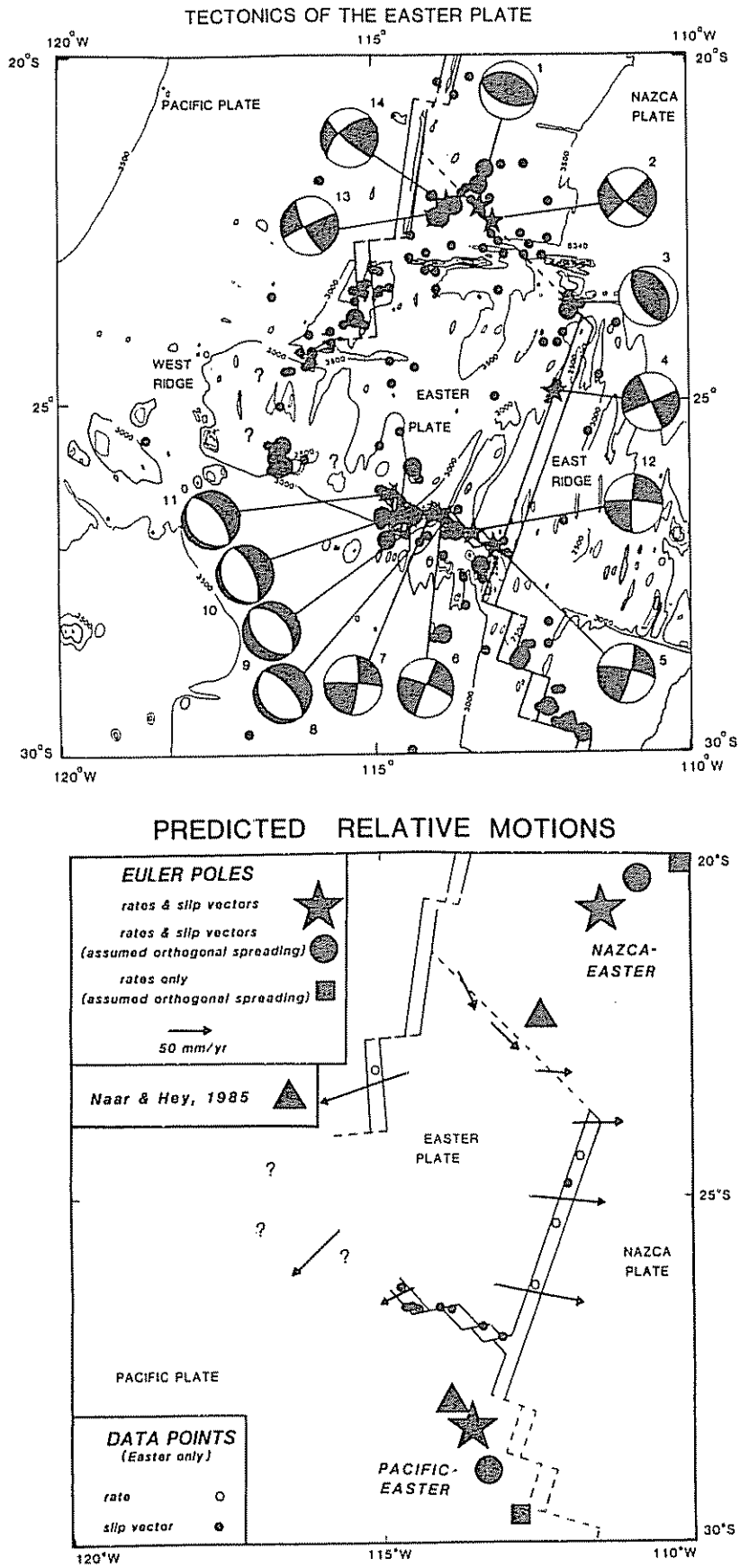

Fig. 8 (Top) Bathymetry, seismicity, and tectonics of the Easter plate. Dots represent earthquake epicenters for the interval 1963-1978; larger dots indicate events with m_b 5.1. The stars represent earthquakes whose mechanisms have been determined. (Bottom) Rigid microplate analysis of the Easter plate system. Euler poles for motions of the Nazca and Pacific plates relative to the Easter plate predicted from inversion of different data sets are indicated. Arrows show the corresponding linear velocities. The open and solid circles represent the locations of rate or slip vector measurements [*Engeln and Stein*, 1984]. Note similarity of Euler poles to preliminary results from a subsequently acquired larger magnetic anomaly data set [*Naar and Hey*, 1985]. This similarity supports the use of such rigid plate motion analysis for microplate systems.

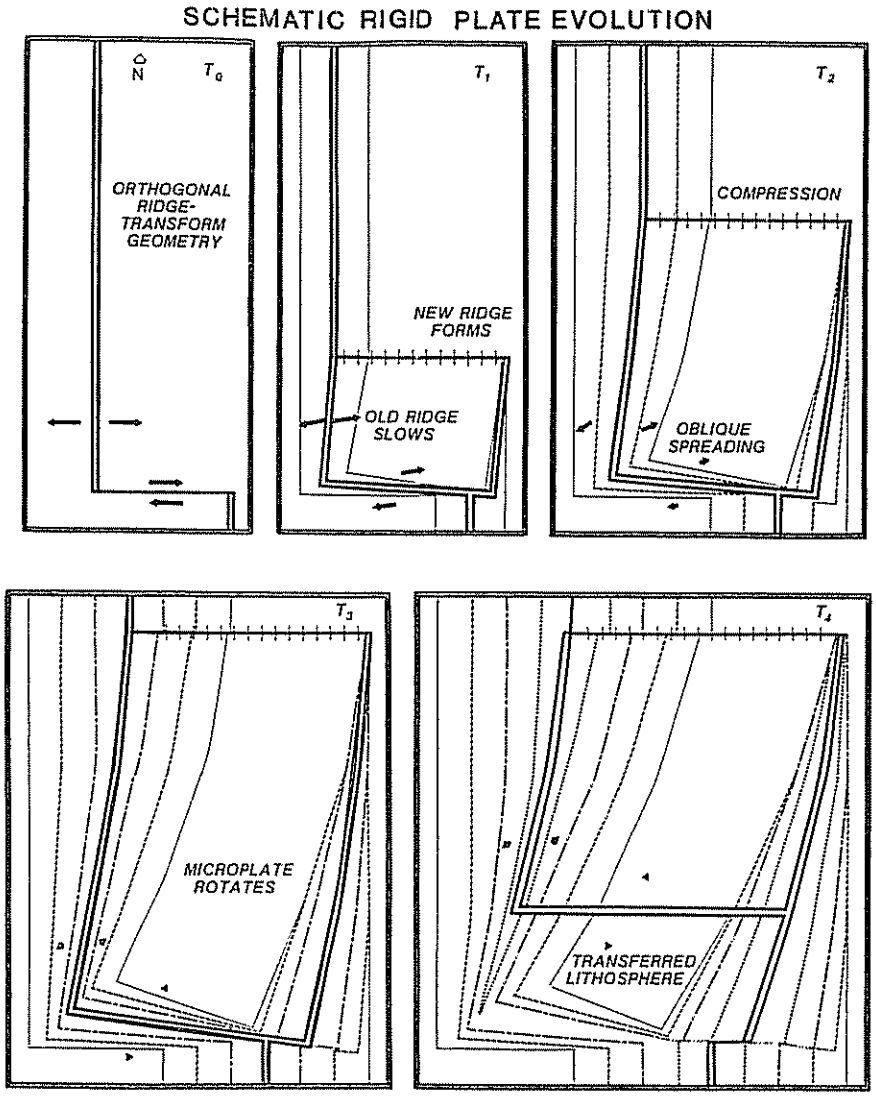

Fig. 9. Evolution of a rigid microplate between two major plates. Note the rotation of the microplate, the reorientation of the two ridges, the formation of a northern converging boundary, and the conversion of the initial transform into a slow spreading ridge. The oldest anomalies on the microplate formed at the growing ridge are pseudofaults. Sets of anomalies formed on the growing and dying ridges "fan" in opposite directions.

constrained by the assumed relative motions, two simple assumptions are made. The propagator tip is joined to the next ridge segment to the north with a straight boundary. Similarly, once the southern boundary begins to propagate northward, it joins the point of zero spreading on the dying ridge to the propagating ridge. For seafloor created on the growing ridge, the boundaries separating preexisting seafloor from that created during propagation are pseudofaults.

The Euler pole for the plate to the east with respect to the microplate is at the propagator tip from time T_0 to T_3, and then migrates northward without further propagation. For simplicity, rift propagation occurs in three discrete time steps. Continuous propagation would smooth the ridge and anomaly orientations.

The isochrons formed on the growing ridge reflect two different aspects of the microplate's history. Rift propagation controls the variation along the growing ridge of the age of the oldest seafloor enclosed within, and thus adjacent to, the pseudofaults. Thus the age of the oldest seafloor formed on the growing ridge during propagation decreases toward the tip, reflecting the more recent initiation of spreading. The position of the Euler pole yields a variation along the growing ridge in spreading rates and hence the distance between successive isochrons. Since in this case the Euler pole is at the rift tip, the spreading rate and hence distance between isochrons increase with distance from the tip. It is worth bearing in mind the differences between the two effects. Although for the case here both effects reinforce to produce the "fanning" anomaly pattern, both need not operate together. It is possible to conceive of rift propagation with a very distant Euler pole, in which case the isochrons would not "fan," but there would be a clear variation in the age of the oldest seafloor enclosed within, and adjacent to, the pseudofaults. Alternatively, a nearby Euler pole could generate a fanning anomaly pattern on a ridge that is not propagating [*Naar and Hey*, 1986, Figure 3].

The sets of anomalies formed on the growing and dying ridges during propagation "fan" in opposite directions. The transform that went into extension also gives rise to "fanned" anomalies. The fanned anomalies leave a characteristic pattern once a piece of lithosphere ceases to be part of the microplate and is transferred to the left plate

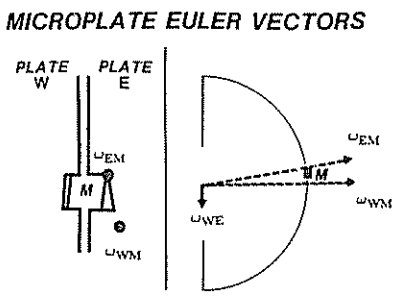

Fig. 10 Geometric constraints on the Euler vectors for a three-plate system: a microplate ("M") between western ("W") and eastern ("E") major plates. If ω_{WE}, the Euler vector for the western major plate relative to the eastern one is far away, and that for the major plate to the east relative to the microplate (ω_{EM}) is near the propagator tip, the magnitude of the latter must be much greater for the spreading rate on the southernmost portion of the propagating rift to be comparable to that between the major plates. As a result, ω_{WM}, the sum of the other two Euler vectors, is similar in both direction and magnitude to ω_{EM}. In this case, since both Euler poles are nearby, relative velocities vary rapidly along all the microplate's boundaries.

(time T_4). The set of fanned anomalies formed on the failed ridge is symmetric about its trace. One half of the set of fanned anomalies formed on the growing ridge remains on the left plate, and the other half moves away on the right plate. As a result, one and a half sets remain on the left plate. *Tamaki and Larson* [this issue] have identified such a pattern in Mesozoic magnetic anomalies in the west central Pacific and interpret it as evidence for the Magellan microplate.

In this context, is it useful to consider the Euler poles for an example similar to what we have been considering. The pole between the major plates is far away, in this example 90°, so that the spreading rate along the ridge between them varies slowly. In contrast, the pole for the motion of the eastern plate relative to the microplate is at the rift tip, so that the spreading rate increases rapidly from zero at the tip. If we require that the spreading rate on the southernmost portion of the propagating rift be comparable to that between the major plates, the magnitude of the Euler vector ω_{EM} for the eastern plate relative to the microplate must be much greater than ω_{WE}, that for the western plate relative to the eastern plate (Figure 10). Since ω_{WM}, the Euler vector for the western plate relative to the microplate, is the sum of the other two Euler vectors, this vector is similar in both magnitude and direction to ω_{EM} and the corresponding Euler pole is also near the microplate, in this case to the south. As a result, the rate of relative motion varies rapidly with distance along the corresponding boundary.

Since the Nazca-Pacific pole is far from both the Easter and Juan Fernandez microplates, then if the Euler pole for the propagating rift is near the tip, such a geometry applies. This is the case for the Euler poles shown for Easter in Figure 8 and for the recent model for Juan Fernandez [*Anderson-Fontana et al.*, 1986]. It appears to have been the case for the Mesozoic Magellan microplate [*Tamaki and Larson*, this issue]. Since the sets of anomalies formed on both of the ridges bounding that microplate fan dramatically, it seems likely that the Euler poles for the microplate's motion relative to both the Farallon and Pacific plates were nearby.

The structural pattern within the microplate reflects several basic effects. Isochrons formed at the growing ridge have been reoriented by the rigid rotation of the microplate. Isochrons formed at the dying ridge have been reoriented by two processes. First, they encounter the migrating northern boundary as they are transferred to the microplate. In the geometry shown, differential contraction occurs, with the maximum shortening furthest from the propagator tip and the minimum shortening at the tip. The resultant differential shortening, shown by comparison of isochron lengths on either side of the west ridge, distorts the fabric somewhat. This effect is especially noticeable in the geometry used for this model, since rates vary rapidly along the northern boundary because the Euler pole is close. Second, once on the microplate, these isochrons rigidly rotate. Thus much of the seafloor within this zone has undergone reorientation, although in the rigid plate model no deformation occurs within the overlap zone.

We have used this rigid case as an approximate analogy to the Easter plate, with time T_3 the present [*Engeln and Stein*, 1984]. As our goal is to trace the evolution of the boundary and structures, we extend the model to a time when some seafloor has shifted from one major plate to the other. In the model (Figure 9), relative motion (arrows) across the dying ridge changes direction with time as the overlap region rigidly rotates. This change can be accommodated in several ways. One (Figure 11) is that as the spreading direction shifts, transforms reorient and remain parallel to the relative motion and ridges propagate and die to maintain a continuous boundary. Here oblique spreading occurs; it is also possible for the ridge segments

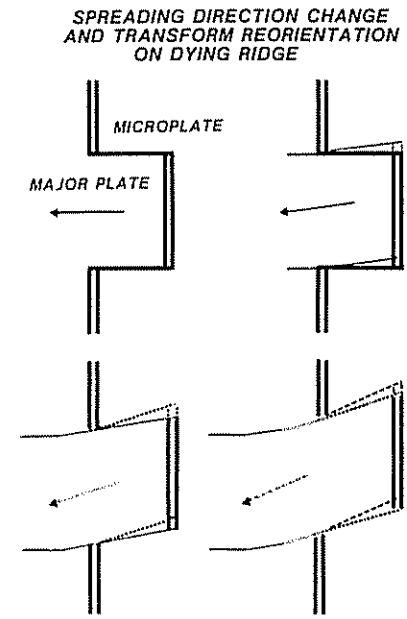

Fig. 11. Spreading direction changes and transform reorientation on a dying ridge. From the initial direction, spreading shifts to a new direction at each time shown. The boundary can adjust in several different ways. In the case shown, transforms reorient to remain parallel to relative plate motion and ridge segments propagate and die to keep the boundary continuous. The boundary adjustment can also occur by formation of leaky transforms or new, orthogonally spreading, ridge segments. Seafloor is constantly broken and transferred from plate to plate by this process.

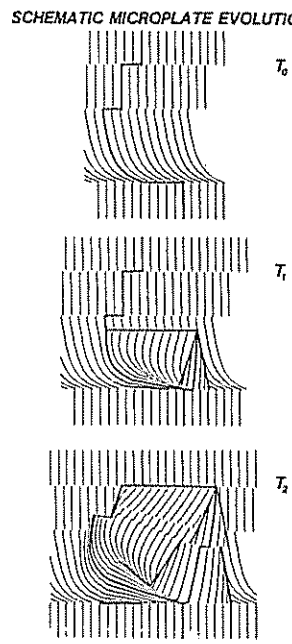

Fig. 12. Schematic evolution of an Easter-type microplate by rift propagation. A new east ridge grows, the west one slows, and the southern transform leaks, becoming a slowly spreading ridge. The microplate interior rotates owing to the variation in spreading rates along the growing ridge. The curved initial geometry is an approximation, since the kinematics allow either oblique or orthogonal spreading on the dying ridge.

to reorient to allow orthogonal spreading or for transforms to retain their orientation and acquire either extensional or contractional components of motion. The relative motion does not constrain which of these will occur; all are acceptable kinematically. Such reorientation may disrupt and complicate the magnetic signature of the ridge, as proposed for the dying ridge at Easter [*Engeln and Stein*, 1984].

As spreading rates and directions can change rapidly along both the propagating and dying ridges, smaller-scale reorientation features may form. *Naar and Hey* [1986] found that the growing ridge at Easter may be composed of several propagating and dying rifts. Moreover, these boundaries may include overlapping spreading centers, as noted at Juan Fernandez [*Craig et al.*, 1983]. Such boundary complexities may make delineation of the active ridges difficult and determination of relative motions less reliable.

In the rigid case, the southern and northern boundaries have a complex evolution required by the change in relative motions along the dual ridges and the constraint that the area between them not deform. Thus these are the boundaries most likely to deviate from this simple geometric model. The southern transform evolves through a "leaky" transform stage [*Menard and Atwater*, 1968] into a nearly orthogonal, slowly spreading ridge by time T_3. At the same time, rotation of the overlap zone about the nearby Euler pole causes convergence across the northern plate boundary, which moves northward with time, reaching its final position at T_3. It would be surprising if the northern boundary evolved exactly like a convergent zone which continuously reforms at new sites, producing some shortening at every point. Nonetheless, we expect that this boundary will be generally convergent. In contrast, the evolution of the initial transform into a slow spreading center is a simpler process and should occur in a fashion similar to the model. It is worth noting that the general nature of the convergent northern and extensional southern boundaries of the Easter plate is similar to this simple model [*Engeln and Stein*, 1984]. In particular, *Hey et al.* [1985] propose that part of the southern boundary is an eastward propagating rift perhaps indicative of a "leaky" transform.

A version of the model with the propagation rate and direction and other kinematic factors closer to the Easter geometry is shown in Figure 12. As propagation occurs, the microplate grows and rotates as the relative motions change. The ridges are shown by heavy lines, pseudofaults are shown dotted, transform faults are shown dashed, and other lines indicate isochrons. As the microplate rotates, spreading occurs on the southwest boundary and shortening induced by the rotation results on the northern boundary. Motion along the dying ridge slows and becomes oblique to the overall ridge trend as propagation continues. Preexisting structures and the ridges are reoriented by purely rigid plate kinematics, both at the propagating boundaries and in the microplate's interior, owing to rigid rotation caused by the differential spreading along the growing and dying ridges. The differential shortening along the migrating northern boundary is reflected within the overlap zone by both isochron length changes and distortion of the original fabric.

Figure 13 compares the last panel of Figure 12 with data for Easter. In general, the fit is good. The trends and relative motions across the boundaries approximate those observed. Structures within the pseudofaults show the observed fanning, and many of the preexisting structures are matched reasonably well both within and outside the microplate. This schematic model, though similar to the Easter geometry, is not a reconstruction, which requires knowledge of the prepropagation geometry and its evolution. The curved initial geometry is a simplification, since the kinematics do not constrain whether the dying ridge spreads obliquely or orthogonally as the direction of motion changes. Moreover, the complex propagation history [*Naar and Hey*, 1986] has been approximated with a single rift that briefly propagated eastward. Nonetheless, the success of the schematic model in reproducing many features of the data suggests that rigid plate kinematics may adequately describe major features resulting from the evolution of microplate systems. We thus suggest that microplate models offer useful testable hypotheses for describing overlap systems and that shear behavior need be invoked only to explain features not describable by rigid plate tectonics.

SHEAR MODELS

We now consider a nonrigid model that, in many ways, resembles the rigid plate geometry of the previous section. Here the entire overlap region deforms in simple shear parallel to the spreading direction as a response to the differential spreading along the growing and dying ridges. Displacement occurs parallel to the original transform orientation and is distributed evenly throughout the overlap region. The model approximates the trend of the pro-

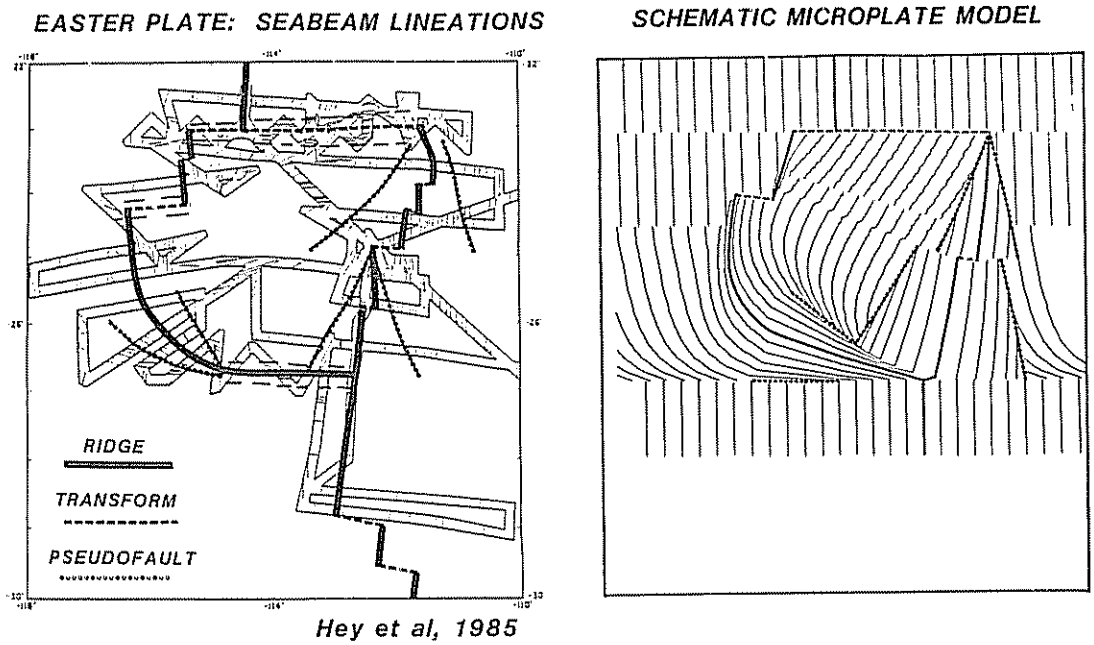

Fig. 13. Comparison of the schematic model (last panel of Figure 12) with Easter plate structural data. The model, though not an actual reconstruction, replicates many of the observed structures. Data along the propagating east ridge and leaky southern boundary are fit reasonably well, as are trends within the major pseudofaults.

pagating rift and the size of the overlap zone (Figure 14). The propagation history, relative plate motion, and initial plate geometry are the same as for the rigid plate model in Figure 9. We show the development of the boundaries of the shear zone to examine the effect of the rigidity of the seafloor within the overlap on the boundary configuration. The spreading rate on the propagating ridge increases linearly with distance from the propagating tip. This is equivalent to having the Euler pole at the tip in the rigid plate case, given the small angle approximation ($\sin\theta = \theta$).

Comparison of Figures 9 and 14 shows significant differences between the rigid plate and simple shear zone cases. In the shear case, isochrons within the overlap zone reorient by differential translation of seafloor. For the rigid case, isochrons within the overlap zone reorient by seafloor transfer at the microplate's boundaries and by rigid rotation. Although the overall trends of the growing and dying ridges are similar, individual segments evolve differently. The rate and direction of motion change along the dying ridge in the rigid case, but in the simple shear case, only the rate changes. In the shear case the direction of relative motion becomes oblique to the overall ridge trend because the ridge reorients as segments further north spread faster than those to the south (Figure 14, arrows). For simplicity the figures show oblique spreading. Because the kinematics determine transform but not ridge orientation, orthogonal spreading is also possible.

The greatest differences between the rigid and simple shear cases are shown by the evolution of the northern and southern boundaries. In contrast to the rigid case, both boundaries remain transforms in the shear case. Motion across the southern boundary slows as spreading slows on the dying ridge. Conversely, motion across the northern transform increases until it becomes a transform between the two large plates and the shear zone vanishes. This shear geometry would predict neither the spreading observed along the southwestern ridge nor the contraction along the northern plate boundary.

This case is a simple shear geometry analogous to that in Figures 4*b* and 6*c*, where rift propagation occurs along isochrons. *McKenzie* [1986] has presented a simple shear model, also for slip parallel to the spreading direction, for a geometry analogous to Figures 4*c* and 6*a*, where rift propagation occurs parallel to the original ridge. For such shear geometries, the evolution of the boundaries and the orientation of structures in the overlap zone differ from the rigid plate model. Other shear geometries are also possible; for example, slip need not be restricted to the spreading direction. R. Hey and D. Naar (personal communication, 1986) suggest that slip may occur along originally ridge-parallel normal faults. Such a geometry, which would exploit preexisting zones of weakness, might produce overlap boundaries and relative motions more similar to the rigid plate geometry. In this geometry, motion in the overlap would be a combination of shear and rotation, analogous to the case discussed by *Nur et al.* [1986], and could allow the southwest ridge to spread under some circumstances.

KINEMATIC FACTORS

For a given initial configuration and direction of propagation, the geometry of the overlap region and the amount of shear or rigid rotation of seafloor within it are determined by a combination of four factors: the propagation rate, the rise time from the initiation of spreading until full spreading is reached, the offset distance between the dual ridges, and the change in spreading rate along each of the dual ridges. The propagation rate times the rise time determines the length of the dual ridges; the offset, which increases with time, determines the width of the overlap zone. Figure 15, drawn for a shear zone case, contrasts

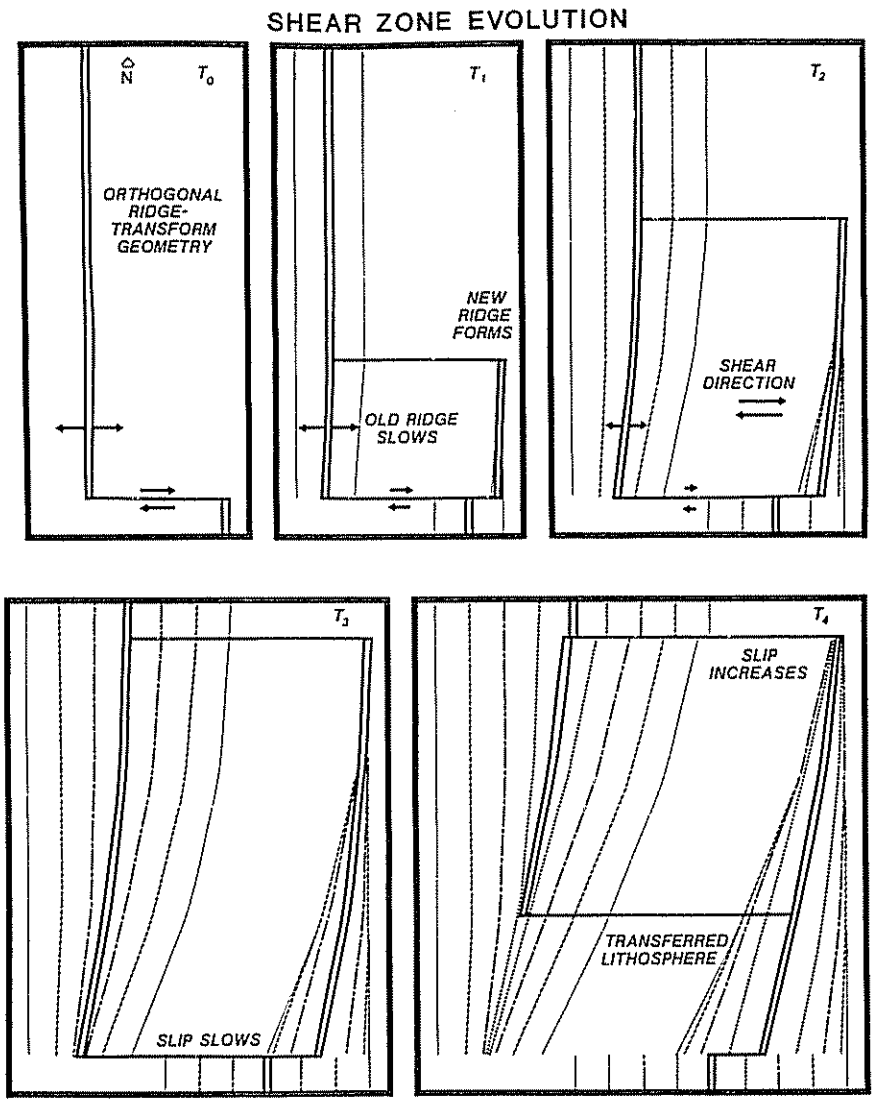

Fig. 14. Evolution of a continuous zone of simple shear between two major plates. Note the internal deformation of the shear zone, the reorientation of the two ridges, and the formation of a northern transform boundary.

the various effects. A greater propagation rate or longer rise time increases the sizes of the overlap region. Thus the most basic propagating rift model is one with zero rise time, such that the two ridges overlap only at a point (Figures 2-6). A finite overlap region occurs for nonzero rise times.

A variety of length to width ratios have been observed in overlap regions. The migration of the Vema Transform, proposed from the identification of abandoned transform valleys [*Van Andel et al.*, 1971] and anomalously old rocks along the flanking ridge [*Bonatti and Crane*, 1982], suggests ratios of about 1 to 5. Overlapping spreading centers are characterized by three to one ratios [*Macdonald et al.*, 1984]. The largest present-day overlap regions, the Easter and Juan Fernandez plates, have intermediate ratios nearer to 1 to 1.

The rate and amount of deformation depend on the propagation rate, rise time, and change in spreading rate over the overlap length. The deformation is shown by the distortion of an initially linear feature, such as the isochron in Figure 15, during and after passage through the shear zone. In this case, the numerical values given are the tangent of the angle from the original orientation or twice the shear strain. The total shear experienced by seafloor transferred from one major plate to the other is inversely proportional to the propagation rate for a given rise time (Figure 15, left and center). Although the rise time does not affect the total shear, a longer rise time results in a slower shear rate but longer residence time in the shear zone, producing the same net deformation (Figure 15, left and right). The amount of shear depends on how rapidly the spreading rate increases along the growing rift.

Relative Plate Motion Inversions

It is natural to ask what occurs if a shear zone overlap system were treated as a rigid plate. In other words, given plate motion data from the boundaries of a shear zone, what would result from inversion of the data? We examine this question using synthetic data for the rigid and simple shear models of the prior sections.

Figure 16 shows the two cases at time T_3, roughly analogous to the present Easter geometry. We assume that

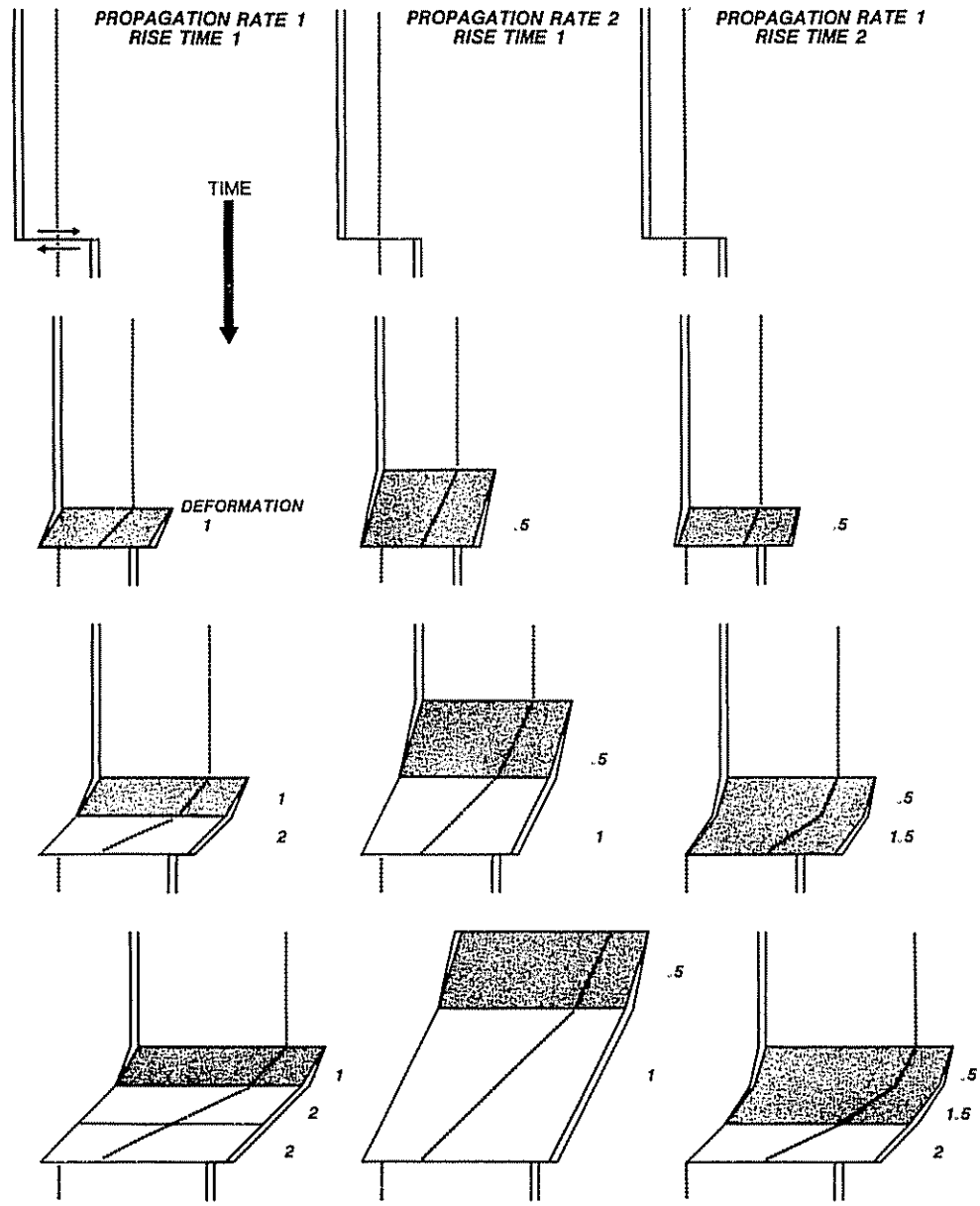

Fig. 15. Effect of ridge propagation rate and rise time on geometry and internal deformation of an overlap region, drawn as a simple shear zone. The active overlap area is shaded. Deformation values, shown by position of the dotted isochron, are twice the shear strain.

rate and azimuth data are available at the points shown, with standard deviations of 1 cm/yr in rate and 10° in azimuth. Stars mark Euler poles determined by inverting the two synthetic data sets using the *Minster et al.* [1974] algorithm. The poles determined for the rigid case are identical to those used to generate the model. The poles found for the shear case correspond to the rigid plate geometry that provides the best fit, in a least squares sense, to the data. Since the data are inappropriate for a rigid model, misfit occurs. The rapid variation in spreading rates favors a nearby pole, while the uniform east-west directions of motion favor a distant pole. The best fitting pole is a compromise between the rate and azimuthal data and is determined by their assigned standard deviations. Comparison of the data (dots) and predictions (dashed line) shows the resulting compromise and misfit. As shown by the shear zone results (Figure 16, right center column), there is an orderly sense of misfit brought about by the conflicting assumptions of a rigid plate analysis performed on nonrigid seafloor.

Additional insight into the results of treating the shear case as rigid can be obtained by examining the north (ridge-ridge-trench) and south (ridge-ridge-ridge) triple junctions in velocity space (Figure 17) [*McKenzie and Morgan*, 1969]. The predictions of motion for the microplate (M) relative to the plates on its west (W) and east (E) can be compared with the "measured" rates and azimuths. For the rigid plate case, the predicted motions fit the data, as expected. In the shear case, the velocity triangle, which is required to close in the inversion because plate rigidity is assumed, incorrectly describes the motion. Point "M (inversion)" gives the predicted position of the microplate in velocity space; point "M (data)" shows its true position. Equivalently, best fit vectors derived for the

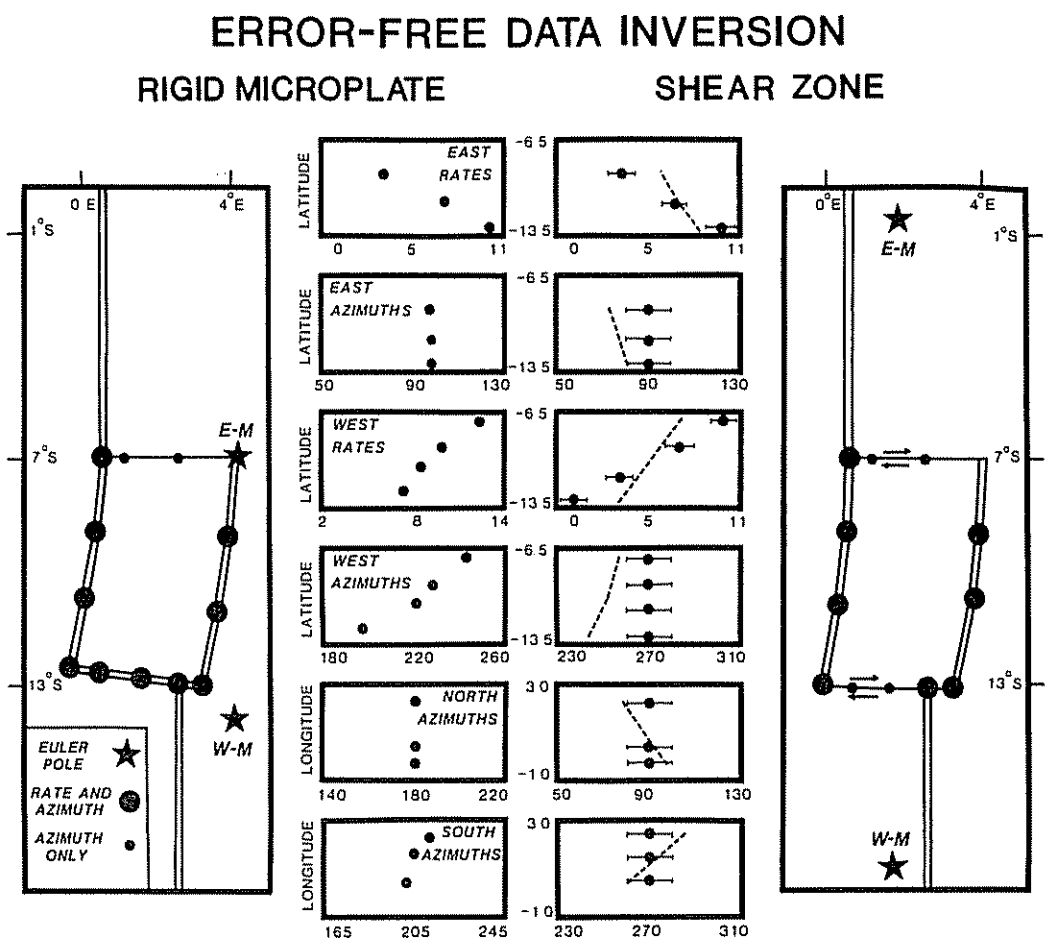

Fig. 16. Relative motion inversion of error free synthetic rate and azimuth data for a three-plate system (a microplate "M" between western "W" and eastern "E" plates) for rigid and simple shear geometries. In the rigid plate case, the data are predicted exactly by the resulting Euler vectors. In the shear case, the data are misfit as the inversion used to calculate the Euler vectors assumes that the plates do not deform internally. The Euler poles are a compromise between the rates, which favor a nearby pole, and the azimuths, which favor a distant one

three plate pairs individually without a closure requirement would fail to close because the rigid plate assumption is invalid

The misfit to the data (Figure 18) indicated by reduced chi-square, χ^2_ν, is, of course, zero for the rigid plate case, and about 1 for the shear case Since the data in both are error free, the only misfit results from the systematic error of treating a shear zone as a rigid plate It is thus more realistic to examine the two cases assuming that errors are present in the data To do so, we conduct 50 numerical experiments in which the data are perturbed by the addition of a Gaussian error to each point This procedure provides an estimate of how the results of a plate motion inversion are affected by errors in the observations [*Stein and Gordon*, 1984] Figure 18 shows a histogram of χ^2_ν for

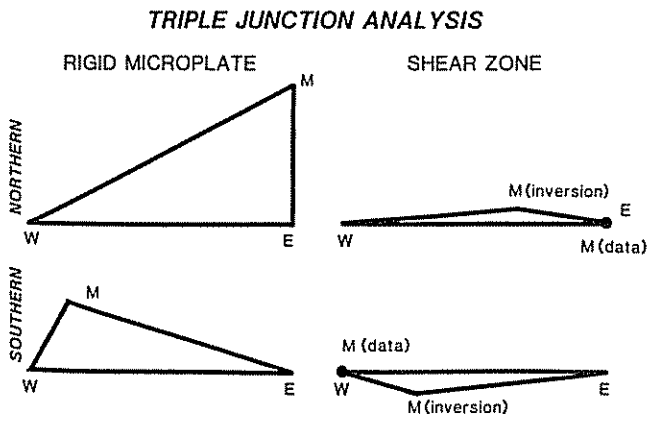

Fig 17. Triple junctions in velocity space for the rigid and shear cases The inversion requires that the junctions close: in the shear case the predicted and observed positions of the microplate disagree

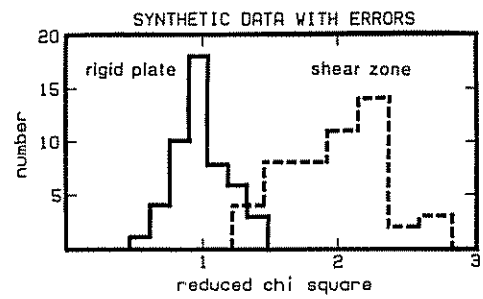

Fig 18. Misfit to relative motion data for the geometry of Figure 16, given Euler vectors resulting from inversion of the data after errors are added. Fifty trials were conducted for each case: the shear case is usually less well fit because the rigid plate assumption is violated

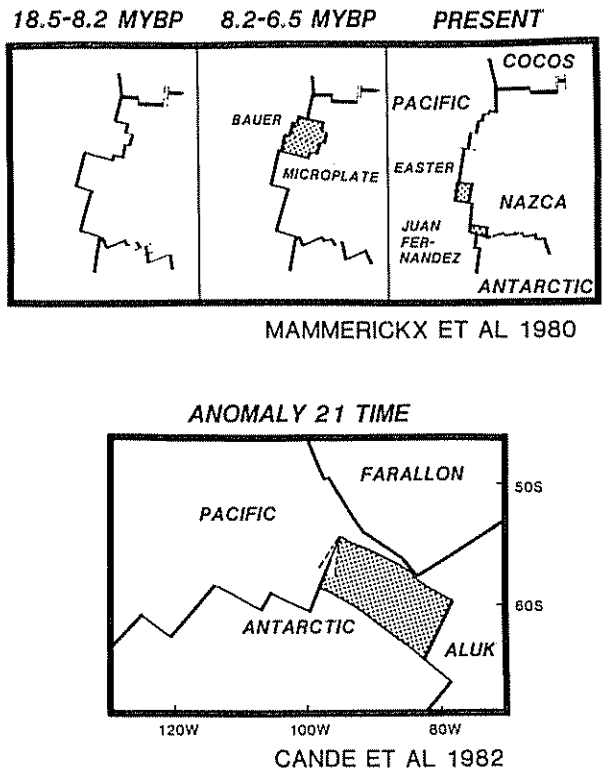

Fig. 19. Microplates associated with past ridge reorganizations (Top) Formation of the Bauer microplate, analogous to the present Easter microplate, during reorganization of the East Pacific Rise. Simplified from *Mammerickx et al.* [1980]. (Bottom) Transfer of a portion of the Pacific plate to the Antarctic plate during northward propagation of the Pacific-Aluk-Antarctic triple junction. If both ridges were simultaneously active, a microplate presumably existed. Note the analogy to the present four-plate system formed by the Juan Fernandez microplate at the Pacific-Nazca-Antarctic triple junction. Simplified from *Cande et al.* [1982].

the two cases. As expected, χ^2_ν is usually about 1 for the rigid case, since the errors are Gaussian with the standard deviations assumed in the inversion. Reduced chi-square is significantly higher, typically about 2, for the shear case as systematic error from the incorrect assumption of rigidity adds to the random errors from the data.

For real data the situation would be more complex, as reduced chi-square is significantly less than 1 for global plate motion models [*Minster and Jordan*, 1978; *Gordon et al.*, 1987], implying that errors in the data are overestimated. As a result, it may be difficult to use reduced chi-square directly to distinguish errors in the data from deviations from plate rigidity. For example, the Easter plate data used in our earlier study [*Engeln and Stein*, 1984] are probably unsuitable. F tests of triple junction misclosure [*Gordon et al.*, 1987] may offer an alternative method of examining possible deviations from plate rigidity in situations where high-quality data are available.

DISCUSSION

The model results have interesting implications for interpretation of data for overlap systems such as the Easter microplate. Most significantly, an oblique structural fabric need not result from pervasive shearing. The Easter data (Figure 13, left) show ridge-parallel north-south trending structures east of the east ridge on the Nazca plate. In contrast, on the microplate west of the ridge the primary structural fabric, oriented northeast-southwest, is oblique to the ridge. A zone of such structures covers much of the plate. More complex patterns appear along the southwest and west ridges, and in the northern interior portion of the plate. Similar patterns can be produced for both rigid (Figures 9, 12, 13) and shear (Figure 14) cases. The structural data are thus consistent with, but do not require, shear within the microplate.

The model results for relative plate motions also have interesting consequences. Most significantly, in a simple shear geometry, neither extension at the south boundary nor shortening at the north boundary occurs. The observations of extensional seismicity [*Engeln and Stein*, 1984] and spreading [*Hey et al.*, 1985] on the southern boundary of the Easter plate and compressive earthquakes near the northern boundary strongly favor a significant component of rigid plate rotation.

Interpretation of the results of the plate motion inversions leads to similar conclusions. In particular, the Euler vectors from our study using earlier data [*Engeln and Stein*, 1984] and the similar preliminary results [*Naar and Hey*, 1985, and personal communication, 1986] from subsequent data predict extension, as observed, on the southern boundary. The inversion used explicitly assumes that the data are on the boundaries of rigid plates and cannot be applied (without major modifications) to a shear zone.

What prospects, then, do these models suggest for studies of the Easter plate and similar situations? The Easter plate geometry is more complex than the schematic model. The model geometry and history were simplified to test the essential ingredient: the effects of shear and rotation on plate boundaries and internal structure. These simulations show that oblique structures in such a geometry are consistent with rigid microplate evolution and may not require pervasive shearing. Such models can be generalized to incorporate more complex geometries and propagation histories as further magnetic and structural data become available. Similarly, the data used in our 1984 study, though adequate for estimation of relative motions, were inadequate to fully test the applicability and limitations of rigid plate models. As improved relative motion and structural fabric data sets become available, better resolution of these issues should be possible.

We thus conclude that a combination of relative motion, seismicity, and structural analyses provides valuable insight into the behavior of the seafloor within large or moderate sized overlap regions. The successful application of these techniques to modern examples suggests that they could also be used to study ancient microplate-sized overlap systems. Studies of past ridge reorganizations suggest that microplates have formed. Figure 19 (top) shows the formation of a possible analog to the present Easter microplate, the Bauer microplate, which existed during an earlier reorganization of the East Pacific Rise [*Mammerickx et al.*, 1980]. Figure 19 (bottom) shows the transfer of a portion of the Pacific plate to the Antarctic plate during a past ridge reorganization [*Cande et al.*, 1982]. Since the transfer was accomplished by northward propagation of the Pacific-Antarctic Ridge while the Aluk-Antarctic Ridge was also active, it seems likely that a microplate (which might be called the Tula plate after the Tula Fracture

Zone which forms its boundary with the Antarctic plate in the figure) existed during rift propagation. The five-plate (microplate plus four major plates) system that resulted from the evolution of the Pacific-Aluk-Antarctic triple junction may have been analogous to the present four-plate system formed by the Juan Fernandez microplate at the Pacific-Nazca-Antarctic triple junction. A microplate model for regions along the Farallon-Pacific Ridge, similar to that for Easter, has been suggested by Sager and Pringle [1987] based on Cretaceous paleomagnetic data from seamounts. Overlaps may also have been associated with events such as the migration of the Vema Transform [*Van Andel et al.*, 1971; *Bonatti and Crane*, 1982]. Analysis of a variety of such systems with various sizes should help define the limits of rigid plate tectonics during ridge reorganizations and provide insights into the relationship of microplates to reorganizations. Possibly microplate models will also prove useful in describing continental rifting in places, such as the Afar triple junction area [*Acton et al.*, 1986], which evolved by rift propagation [*Courtillot et al.*, 1980].

The analysis presented here offers no direct way of assessing when shear or rigid behavior will occur. One might expect more rigid, platelike tectonics at larger overlap systems owing to the increase in lithospheric thickness and strength with age. Analysis of a variety of overlap geometries will show if these generalizations in fact apply.

Single ridge spreading systems are obviously the norm. Simple energy arguments show that dual ridge systems are not, in general, favored [*Sleep et al.*, 1979]. Nonetheless, under certain conditions, dual ridge systems do evolve. Local effects such as hotspots [*Hey and Vogt*, 1977; *Hey et al.*, 1985], triple junction geometries [*Cande et al.*, 1982; *Rea and Dixon*, 1983; *Anderson-Fontana et al.*, 1986; *Tamaki and Larson*, this issue], and fast spreading [*Hey et al.*, 1985] may play a role in many overlap systems. Overlap systems are intimately related to major ridge reorganizations, since overlaps are often produced when ridge geometries changed. It is, however, unclear whether overlap systems are general features of ridges that can form under a wide range of circumstances or whether they are characteristic of certain, limited intervals when significant changes in the plate boundary configuration are occurring. For example, do the nearby Easter and Juan Fernandez plates reflect a present ridge reorientation, or are they caused by purely local (hotspot and triple junction) effects? Detailed study of both modern and ancient overlap systems should help resolve this issue.

Acknowledgments. We thank Sandra Anderson-Fontana, Rodey Batiza, Allan Cox, Richard Hey, Roger Larson, David Naar, and Roger Searle for useful discussions. This research was supported by NSF grants EAR 8407510 and 8417323 and NASA Crustal Dynamics grant NAG5-885. Acknowledgment is also made to the donors of the Petroleum Research Fund, administered by the American Chemical Society, for partial support of this research.

REFERENCES

Acton, G., J. Werner, S. Stein, and J. Engeln, Propagating rift models of plate boundary evolution at the Afar triple junction in eastern Africa (abstract), *Eos Trans. AGU, 67*, 1209, 1986.

Anderson, R. N., D. W. Forsyth, P. Molnar, and J. Mammerickx, Fault plane solutions of earthquakes on the Nazca plate boundaries and the Easter plate, *Earth Planet. Sci. Lett., 24*, 188-202, 1974.

Anderson-Fontana, S., J. F. Engeln, P. Lundgren, R. L. Larson, and S. Stein, Tectonics and evolution of the Juan Fernandez microplate at the Pacific-Nazca-Antarctic triple junction, *J. Geophys. Res., 91*, 2005-2018, 1986.

Bonatti, E., and K. Crane, Oscillatory spreading explanation of anomalously old uplifted crust near oceanic transforms, *Nature, 300*, 343-345, 1982.

Cande, S. C., E. M. Herron, and B. R. Hall, The early Cenozoic history of the southeast Pacific, *Earth Planet. Sci. Lett., 57*, 63-74, 1982.

Chase, C. G., The N plate problem of plate tectonics, *Geophys. J. R. Astron. Soc., 29*, 117-122, 1972.

Courtillot, V., Propagating rifts and continental breakup, *Tectonics, 1*, 239-250, 1982.

Courtillot, V., A. Galdeano, and J. L. Le Mouel, Propagation of an accreting plate boundary: A discussion of new aeromagnetic data in the Gulf of Tadjurah and southern Afar, *Earth Planet. Sci. Lett., 47*, 144-160, 1980.

Craig, H., K. R. Kim, and J. Francheteau, Active ridge crest mapping on the Juan Fernandez micro-plate: The use of seabeam-controlled hydrothermal plume surveys (abstract), *Eos Trans. AGU, 64*, 856, 1983.

Engeln, J. F., and S. Stein, Tectonics of the Easter plate, *Earth Planet. Sci. Lett., 68*, 259-270, 1984.

Forsyth, D. W., Mechanisms of earthquakes and plate motions in the East Pacific, *Earth Planet. Sci. Lett., 17*, 189-193, 1972.

Gordon, R. G., S. Stein, C. DeMets, and D. F. Argus, Statistical tests for the closure of plate motion circuits, *Geophys. Res. Lett., 14*, 587-590, 1987.

Gutenberg, B., and C. F. Richter, *Seismicity of the Earth and Associated Phenomena (2nd ed.)*, Princeton University Press, Princeton, NJ, 1954.

Handschumacher, D. W., R. H. Pilger, Jr., J. A. Foreman, and J. F. Campbell, Structure and evolution of the Easter plate, Nazca Plate: Crustal Formation and Andean Convergence, *Mem. Geol. Soc. Am. 154*, 63-76, 1981.

Herron, E. M., Two small crustal plates in the South Pacific near Easter Island, *Nature Phys. Sci., 240*, 35-37, 1972.

Hey, R., A new class of "pseudofaults" and their bearing on plate tectonics: A propagating rift model, *Earth Planet. Sci. Lett., 37*, 321-325, 1977.

Hey, R., and P. Vogt, Spreading center jumps and sub-axial asthenosphere flow near the Galapagos hotspot, *Tectonophysics, 37*, 41-52, 1977.

Hey, R. N., and D. S. Wilson, Propagating rift explanation for the tectonic evolution of the Northeast Pacific—the pseudomovie, *Earth Planet. Sci. Lett., 58*, 167-188, 1982.

Hey, R., F. K. Duennebier, and W. J. Morgan, Propagating rifts on mid-ocean ridges, *J. Geophys. Res., 85*, 3647-3658, 1980.

Hey, R. N., D. F. Naar, M. C. Kleinrock, W. J. P. Morgan, E. Morales, and J.-G. Schilling, Microplate tectonics along a superfast seafloor spreading system near Easter Island, *Nature, 317*, 320-325, 1985.

Hey, R. N., M. C. Kleinrock, S. P. Miller, T. M. Atwater, and R. C. Searle, Sea Beam/Deep-tow investigation of an active oceanic propagating rift system, Galapagos 95.5° W, *J. Geophys. Res., 91*, 3369-3393, 1986.

Isezaki, N., and S. Uyeda, Geomagnetic anomaly pattern of the Japan Sea, *Mar. Geophys. Res., 2*, 51-59, 1973.

Macdonald, K. C., and P. J. Fox, Overlapping spreading centres: New accretion geometry on the East Pacific Rise, *Nature, 302*, 55-58, 1983.

Macdonald, K. C., J. -C. Sempere, and P. J. Fox, East Pacific Rise from Siqueiros to Orozco Fracture Zones: Along-strike continuity of axial neovolcanic zone and structure and evolution of overlapping spreading centers, *J. Geophys. Res., 89*, 6049-6069, 1984.

Madsen, J. A., K. C. Macdonald, and P. J. Fox, Morphotectonic fabric of the Orozco Fracture Zone: Results from a sea beam investigation, *J. Geophys. Res., 91*, 3439-3454, 1986.

Mammerickx, J., and S. M. Smith, Bathymetry of the southeast Pacific, *Geol. Soc. Am. Map Chart Ser., MC-26*, 1978.

Mammerickx, J., E. Herron, and L. Dorman, Evidence for two fossil spreading ridges in the southeast Pacific, *Geol. Soc. Am. Bull., 91*, 263-271, 1980.

McKenzie, D. P., The geometry of propagating rifts, *Earth Planet. Sci. Lett., 77*, 176-186, 1986.

McKenzie, D. P., and W. J. Morgan, Evolution of triple junctions, *Nature, 224,* 125-133, 1969.

Menard, H. W., Sea Floor Relief and Mantle Convection, *Physics and Chemistry of the Earth, 6,* 315-364, 1966.

Menard, H. W., Fragmentation of the Farallon plate by pivoting subduction, *J. Geol., 86,* 99-110, 1978.

Menard, H. W., and T. Atwater, Changes in direction of sea-floor spreading, *Nature, 219,* 463-467, 1968.

Menard, H. W., T. E. Chase, and S. M. Smith, Galapagos Rise in the southeast Pacific, *Deep-Sea Res., 11,* 233-244, 1964.

Minster, J. B., and T. H. Jordan, Present-day plate motions, *J. Geophys. Res., 83,* 5331-5354, 1978.

Minster, J. B., T. H. Jordan, P. Molnar, and E. Haines, Numerical modeling of instantaneous plate tectonics, *Geophys. J. R. Astron. Soc., 36,* 541-576, 1974.

Naar, D. F., and R. N. Hey, Possible models for the origin and evolution of the Easter microplate (abstract), *Eos Trans. AGU, 66,* 968, 1985.

Naar, D. F., and R. N. Hey, Fast rift propagation along the East Pacific Rise near Easter Island, *J. Geophys. Res., 91,* 3425-3438, 1986.

Nur, A., H. Ron, and O. Scotti, Fault mechanics and the kinematics of block rotations, *Geology, 14,* 746-749, 1986.

Okal, E. A., and J.-M. Bergeal, Mapping the Miocene Farallon Ridge Jump on the Pacific plate: A seismic line of weakness, *Earth Planet. Sci. Lett., 63,* 113-122, 1983.

Phipps Morgan, J., and E. M. Parmentier, Causes and rate-limiting mechanisms of ridge propagation: A fracture mechanics model, *J. Geophys. Res., 90,* 8603-8612, 1985.

Rea, D. K., and J. M. Dixon, Late Cretaceous and Paleogene tectonic evolution of the North Pacific Ocean, *Earth Planet. Sci. Lett., 65,* 145-166, 1983.

Sager, W. W., and M. S. Pringle, Paleomagnetic constraints on the origin and evolution of the Musicians and South Hawaiian Seamounts, Central Pacific Ocean, in *Seamounts, Islands and Atolls, Geophys. Monogr.,* edited by R. Batiza, B. Keating, P. Fryer and G. Bohlert, AGU, Washington, D.C., in press, 1986.

Schilling, J.-G., H. Sigurdsson, A. N. Davis, and R. N. Hey, Easter microplate evolution, *Nature, 317,* 325-331, 1985.

Searle, R. C., and R. N. Hey, Gloria observations of the propagating rift at 95.5°W on the Cocos-Nazca spreading center, *J. Geophys. Res., 88,* 6433-6448, 1983.

Sleep, N. H., S. Stein, R. J. Geller, and R. G. Gordon, Comment on "The use of the minimum-dissipation principle in tectonophysics," *Earth Planet. Sci. Lett., 45,* 218-220, 1979.

Stein, S., and R. Gordon, Statistical tests of additional plate boundaries from plate motion inversions, *Earth Planet. Sci. Lett., 69,* 401-412, 1984.

Tamaki, K., and R. L. Larson, The Mesozoic history of the Magellan microplate in the western central Pacific, *J. Geophys. Res.,* this issue.

Van Andel, T. H., R. P. Von Herzen, and J. D. Phillips, The Vema Fracture Zone and the tectonics of transverse shear zones in oceanic crustal plates, *Mar. Geophys. Res., 1,* 261-283, 1971.

Wilson, D. S., R. N. Hey, and C. Nishimura, Propagation as a mechanism of reorientation of the Juan de Fuca Ridge, *J. Geophys. Res., 89,* 9215-9225, 1984.

J. F. Engeln, Department of Geology, University of Missouri, Columbia, MO 65211.

R. G. Gordon, S. Stein, and J. Werner, Department of Geological Sciences, Northwestern University, Evanston, IL 60208.

(Received October 10, 1985;
revised March 6, 1987;
accepted March 30, 1987.)